

Multivariate Analyses of Amyloid-Beta Oligomer Populations Indicate a Connection between Pore Formation and Cytotoxicity

Panchika Prangkio¹, Erik C. Yusko¹, David Sept^{1,2}, Jerry Yang³, Michael Mayer^{1,4*}

1 Department of Biomedical Engineering, University of Michigan, Ann Arbor, Michigan, United States of America, **2** Center for Computational Medicine and Bioinformatics, University of Michigan, Ann Arbor, Michigan, United States of America, **3** Department of Chemistry and Biochemistry, University of California San Diego, La Jolla, California, United States of America, **4** Department of Chemical Engineering, University of Michigan, Ann Arbor, Michigan, United States of America

Abstract

Aggregates of amyloid-beta (A β) peptides are thought to be involved in the development of Alzheimer's disease because they can change synaptic plasticity and induce neuronal cell death by inflammation, oxidative damage, and transmembrane pore formation. Exactly which oligomeric species underlie these cytotoxic effects remains unclear. The work presented here established well-controlled aggregation conditions of A β _{1–40} or A β _{1–42} peptides over a 20-day period and characterized these preparations with regard to their β -sheet content, degree of fibril formation, relative abundance of various oligomer sizes, and propensity to induce membrane pore formation and cytotoxicity. Using this multivariate data set, a systematic and inherently unbiased partial least squares (PLS) approach showed that for both peptides the abundance of oligomers in the tetramer to 13-mer range contributed positively to both pore formation and cytotoxicity, while monomers, dimers, trimers, and the largest oligomers (>210 kDa) were negatively correlated to both phenomena. Multivariate PLS analysis is ideally suited to handle complex data sets and interdependent variables such as relative oligomer concentrations, making it possible to elucidate structure function relationships in complex mixtures. This approach, therefore, introduces an enabling tool to the field of amyloid research, in which it is often difficult to interpret the activity of individual species within a complex mixture of bioactive species.

Citation: Prangkio P, Yusko EC, Sept D, Yang J, Mayer M (2012) Multivariate Analyses of Amyloid-Beta Oligomer Populations Indicate a Connection between Pore Formation and Cytotoxicity. PLoS ONE 7(10): e47261. doi:10.1371/journal.pone.0047261

Editor: Jie Zheng, University of Akron, United States of America

Received: July 25, 2012; **Accepted:** September 7, 2012; **Published:** October 15, 2012

Copyright: © 2012 Prangkio et al. This is an open-access article distributed under the terms of the Creative Commons Attribution License, which permits unrestricted use, distribution, and reproduction in any medium, provided the original author and source are credited.

Funding: This work was supported by the Wallace H. Coulter Foundation (M.M.). J.Y. acknowledges support from the Alzheimer's Association (NIRG-08-01651) and an NSF CAREER Award to J.Y. (CHE-0847530). P.P. is supported by government of Thailand. The funders had no role in study design, data collection and analysis, decision to publish, or preparation of the manuscript.

Competing Interests: The authors have declared that no competing interests exist.

* E-mail: mimayer@umich.edu

Introduction

Alzheimer's disease (AD) is characterized by the accumulation of amyloid- β (A β) peptide aggregates and the formation of insoluble plaques in the brain of affected patients [1–3]. The major components of these amyloid plaques are A β peptides with 40 (A β _{1–40}) and 42 amino acids (A β _{1–42}), both of which are thought to play an important role in AD pathogenesis [4–9]. The pathogenic mechanisms leading to AD are, however, not well understood and several hypotheses are being actively investigated [10–13]. These hypotheses are based on evidence that oligomeric A β peptides can change synaptic plasticity [9,14–20] or cause neurotoxicity [21] by triggering inflammatory responses, oxidative damage [9], dysregulation of ion homeostasis (including Ca²⁺ ions) [2,22], and altered kinase and phosphatase activities that can lead to neurofibrillary tangles [23–25].

With regard to the sizes of A β oligomers that might be the most important for the pathogenesis of AD, several *in vitro* neurotoxicity [26] and *in vivo* studies in mouse models of AD [27] implicated the following oligomers: dimers [28–34], trimers [35], tetramers to 9-mers (also called A β -derived diffusible ligands, ADDLs, with an estimated mass of 17–42 kDa) [16,36–39], 12-mers [15] also called A β *56 [39,40], and protofibrils containing

aggregates larger than 100 kDa, which correspond to 22-mers and bigger aggregates [41–44]. In addition to these oligomeric species, several studies have revealed that insoluble A β fibrils induce neurotoxicity and impair synaptic transmission [21,45–47].

Pore formation by A β is one plausible mechanism for toxicity and for antimicrobial peptide (AMP) activity [48], since oligomeric A β binds to lipid membranes [49,50] and since A β -induced pores could result in aberrant flux of Ca²⁺ ions and cause cell death [6,22,51–55]. For instance, Soscia et al. showed recently that A β acts as an AMP against eight clinically relevant microorganisms and that brain homogenates of AD patients were significantly more antimicrobial than homogenates from age-matched control samples [48]. Various biochemical, biophysical, and computational techniques have indicated a range of aggregated A β species that could potentially induce pores or form ion channel-like structures in artificial lipid bilayers and in neuronal membranes [54,56–59]. For instance, Jang et al. performed molecular dynamics (MD) simulations and proposed that 16- to 24-mers of A β arrange into pore-like structures [60], which are compatible with the dimensions and shape of putative A β pore structures obtained from atomic force microscopy (AFM) [61,62]. In two separate MD studies, Strodel et al. identified tetramers or hexamers as the most stable structures that could form A β pores [63], while Shafir et al.

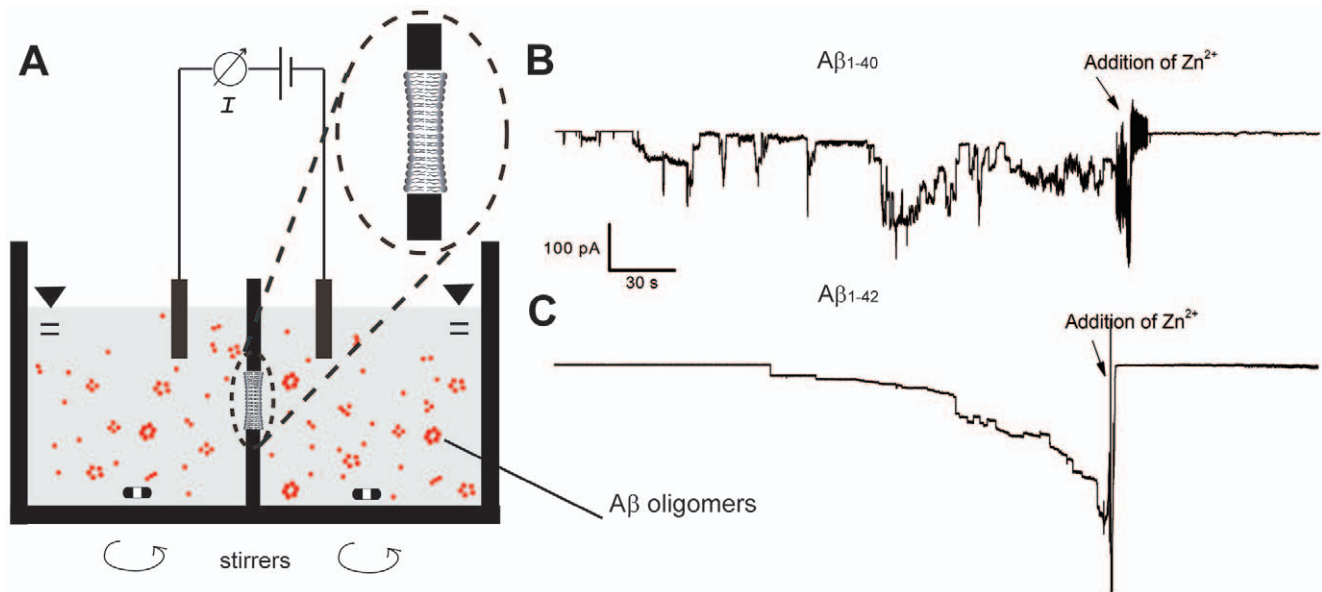


Figure 1. Pore formation by $A\beta_{1-40}$ and $A\beta_{1-42}$ in planar lipid bilayers. **A)** Cartoon of the experimental setup. **B)** Example of transmembrane ion flux induced by 15 μM $A\beta_{1-40}$ prepared by one day incubation in water (method A, Table S1). **C)** Example of transmembrane current induced by 15 μM $A\beta_{1-42}$ prepared by three day incubation (method A). Addition of 10 mM Zn^{2+} (arrows) inhibited $A\beta$ -induced ion flux. doi:10.1371/journal.pone.0047261.g001

suggested that $A\beta$ pores contain assemblies of six hexamers (i.e. a 36-mer) [64]. Based on mass spectrometry, Pan et al. recently revealed β -barrels of tetrameric $A\beta_{1-40}$ peptides arranged in antiparallel β -turn- β motifs [65]. Demuro et al. demonstrated on *Xenopus* oocytes that $A\beta_{1-42}$ oligomers in the range from 5- to 40-mers caused Ca^{2+} flux that was independent of endogenous ion channels [44]. Schauerte et al. combined single molecule fluorescence microscopy with ion current recordings and reported that hexamers were the smallest oligomeric $A\beta$ structure that could permeabilize lipid membranes, while 12- to 14-mers resulted in pores with the largest conductivity for ions [66]. This work is particularly relevant since it was carried out with $A\beta$ concentrations in the nanomolar range and, therefore, close to the concentrations of $A\beta$ observed in human brains [67]. In addition, assays with liposomes showed dye leakage in the presence of $A\beta$ oligomers and reduced leakage in the presence of fibrils [49]. Laganowsky et al. showed recently that a segment of the amyloid-forming protein $\alpha\beta$ crystallin can form cylindrical barrels with an open central channel from six antiparallel proteins and that this so-called cylindrical structure is compatible with a sequence element from $A\beta$ [68]. Lashuel et al. showed by electron microscopy that a mutant version of $A\beta$ that is associated with early-onset Alzheimer's disease, called $A\beta_{\text{ARC}}$, formed pore-like assemblies from 40 to 60 monomers [69], while recent X-ray diffraction and electron microscopy studies showed that these pore-like assemblies may be formed by 20-mers of $A\beta_{1-42}$ with cross- β architecture [70].

Here, we established a well-controlled and reproducible preparation method to form $A\beta$ aggregates over 0, 1, 2, 3, 10 and 20 days in water. We examined the ability of these populations to form ion pores in planar lipid bilayers and separately quantified their cytotoxic effects on a human neuroblastoma cell line. For each time point during the aggregation process, we quantified the relative abundance of different $A\beta$ oligomers and correlated individual oligomer levels with pore formation and toxicity data as well as with β -sheet content and degree of fibrillization. We carried out all assays with the same $A\beta$ preparation at each time point in

order to enable a systematic study of cross-correlation of abundance of oligomer species in two $A\beta$ preparations ($A\beta_{1-40}$ and $A\beta_{1-42}$) with the propensity of the same preparations to form pores and cause cell death. To make this analysis quantitative, we adopted a partial least squares (PLS) approach and found that cytotoxicity and pore formation have identical dependencies on the oligomer distribution, supporting a causative relationship between these phenomena.

Results and Discussion

Probability of Pore Formation is Maximal after Incubating $A\beta$ Samples for 2–3 Days

Figure 1 illustrates that both $A\beta_{1-40}$ and $A\beta_{1-42}$ caused channel-like ion flux across planar lipid bilayers that could be inhibited by Zn^{2+} ions, as reported previously [51,53,54,61,62,71–78]. The conductance values of these recorded current modulations were not well defined and typically ranged from 80 pS to 0.8 nS, while their open pore lifetimes ranged from milliseconds to several minutes as reported previously [79]. These biophysical characteristics of $A\beta$ -induced transmembrane current flux suggest that $A\beta$ may either self-assemble to a transmembrane protein pore, reminiscent of ion channel proteins [71] or $A\beta$ may interact with lipid membranes [49,50,80] and induce defects in the membrane, reminiscent of certain antimicrobial peptides [48,54,67]. It is also possible that both mechanisms act in parallel. In the context of this work, we chose the terminology “ $A\beta$ -induced ion flux” or “pore formation” in order to include both possibilities.

Since aggregation conditions affect the aggregation kinetics and potentially the morphology of $A\beta$ aggregates, we compared five different aggregation methods of $A\beta$ samples from various suppliers for their ability to form pores in planar lipid bilayers (Supporting Information, Table S1, Methods A–E and Figure S1, S2, and S3). Among these methods, we selected incubation of $A\beta$ samples in water for 0 to 20 days (Method A) because it made it possible to study the effects of $A\beta$ aggregation on pore formation over time while being compatible with assays for cytotoxicity, CD

spectroscopy, and ThT fluorescence assays (see Supporting Information Section S2.2 for a comparison and discussion of these five methods for A β aggregation).

Fig. 2A shows that the probability of pore formation was highest when A β samples were pre-incubated in water for 2–3 d in the case of A β _{1–40} or for 2 d in the case of A β _{1–42}. In contrast, pore formation was least likely when A β samples were pre-incubated for 0 d or 20 d. With regard to the biophysical characteristics of A β -induced ion flux, we did not observe consistent differences in the conductance or lifetime of ion flux events among different aggregation methods (A–E, Table S1). In fact, the conductance and lifetime of A β -induced pores varied significantly between experiments with the same preparation method or within the 30 min of one experiment. This variability suggests that A β -induced pores are dynamic structures with a range of conformations and sizes [79]. Control experiments without A β revealed ion flux in one of eleven experiments; this activity was likely due to a sporadic instability of bilayers within the 30 min recording period; these instabilities can occur during bilayer recordings [81].

Cytotoxicity is Maximal after Aggregating A β _{1–40} for Three to Ten Days and A β _{1–42} for Two to Ten Days

Samples of A β resulted in maximal cytotoxicity in a human neuroblastoma cell line after incubating A β _{1–40} for three to ten days, while the toxicity of A β _{1–42} was highest between two and ten days (Fig. 2B). Wogulis et al. found a similar time-dependent trend of toxicity albeit under different conditions and therefore different

kinetics [82]. For information on the toxicity of all A β preparation methods explored here, see Table S1.

Oligomer Levels during Aggregation

In order to correlate both pore formation and cytotoxicity with the aggregation state of A β samples, we determined the relative abundance of monomeric and oligomeric species of A β as a function of incubation time in water. Choosing among the available analytical methods, which all have their limitations [67], we selected SDS-PAGE separation of cross-linked A β samples combined with Western blotting (Fig. 3) and densitometry for this quantification (i.e., analysis of grey levels from scanned images of Western blotted gels). This approach yielded the resolution of individual oligomer species or groups of oligomers as indicated in Fig. 3A (see Supporting Information, Section S2.4 and S2.5 for a discussion on using Western blot for this analysis).

Figure 3B shows that the relative abundance of low molecular weight aggregates (i.e., monomers to trimers) decreased as a function of aggregation time, whereas the relative abundance of intermediate-sized oligomers (tetramers to 13-mers in the case of A β _{1–40} and tetramers to hexamers in the case of A β _{1–42}) went through a maximum after approximately 2 to 3 days. We observed, as expected, that the relative abundance of high molecular weight oligomers (>18-mers) gradually increased over time.

Since the binding of anti-A β antibodies to oligomers could be conformation dependent, we compared the results from densi-

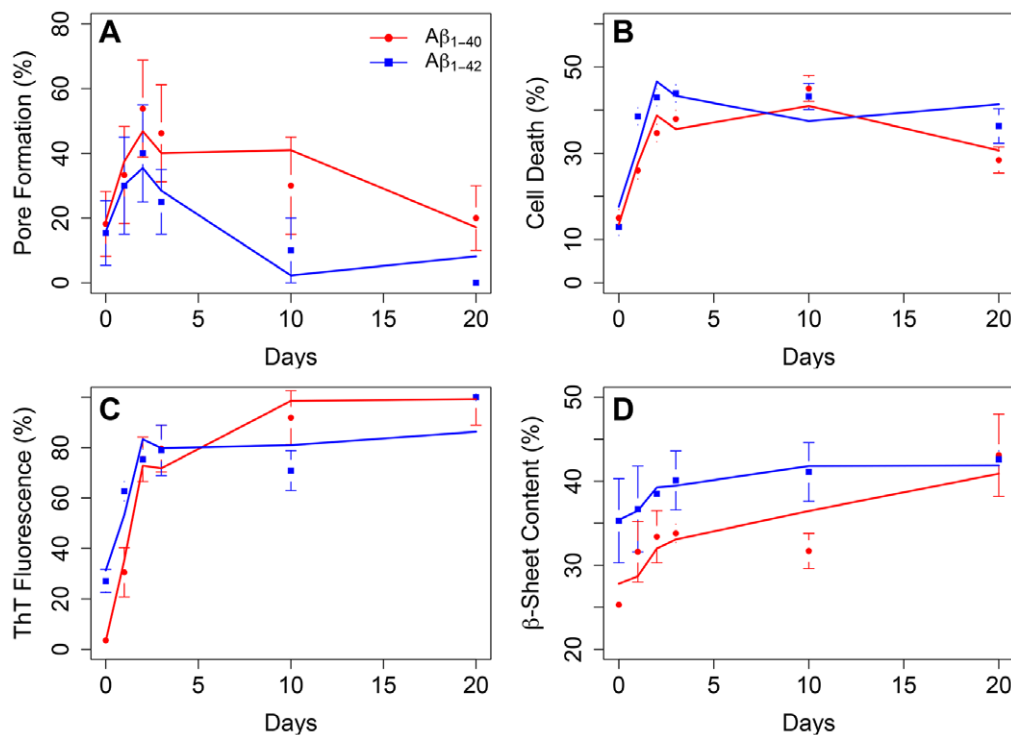


Figure 2. Pore formation, cytotoxicity, ThT fluorescence and β -sheet content as a function of aggregation time of A β samples in water (method A). Red and blue curves in each panel are the two component predictions from PLS regression for A β _{1–40} or A β _{1–42}, respectively. **A)** Percentage of experiments that showed pore formation in planar lipid bilayers. Each point represents 10–15 experiments in the presence of 15–25 μ M A β _{1–40} or A β _{1–42}; error bars represent the error of proportion. **B)** Cell death of human neuroblastoma SH-SY5Y cells 24 h after exposure to serum-free media containing 20 μ M A β prepared by method A. Each point represents 5–15 independent experiments. **C)** Degree of fibril formation as determined by ThT fluorescence. Each point represents an average from 5–20 experiments, error bars represent standard errors of the mean. **D)** Beta-sheet formation as determined by CD spectroscopy. Each point represents an average from 3–5 experiments, error bars represent standard errors of the mean.

doi:10.1371/journal.pone.0047261.g002

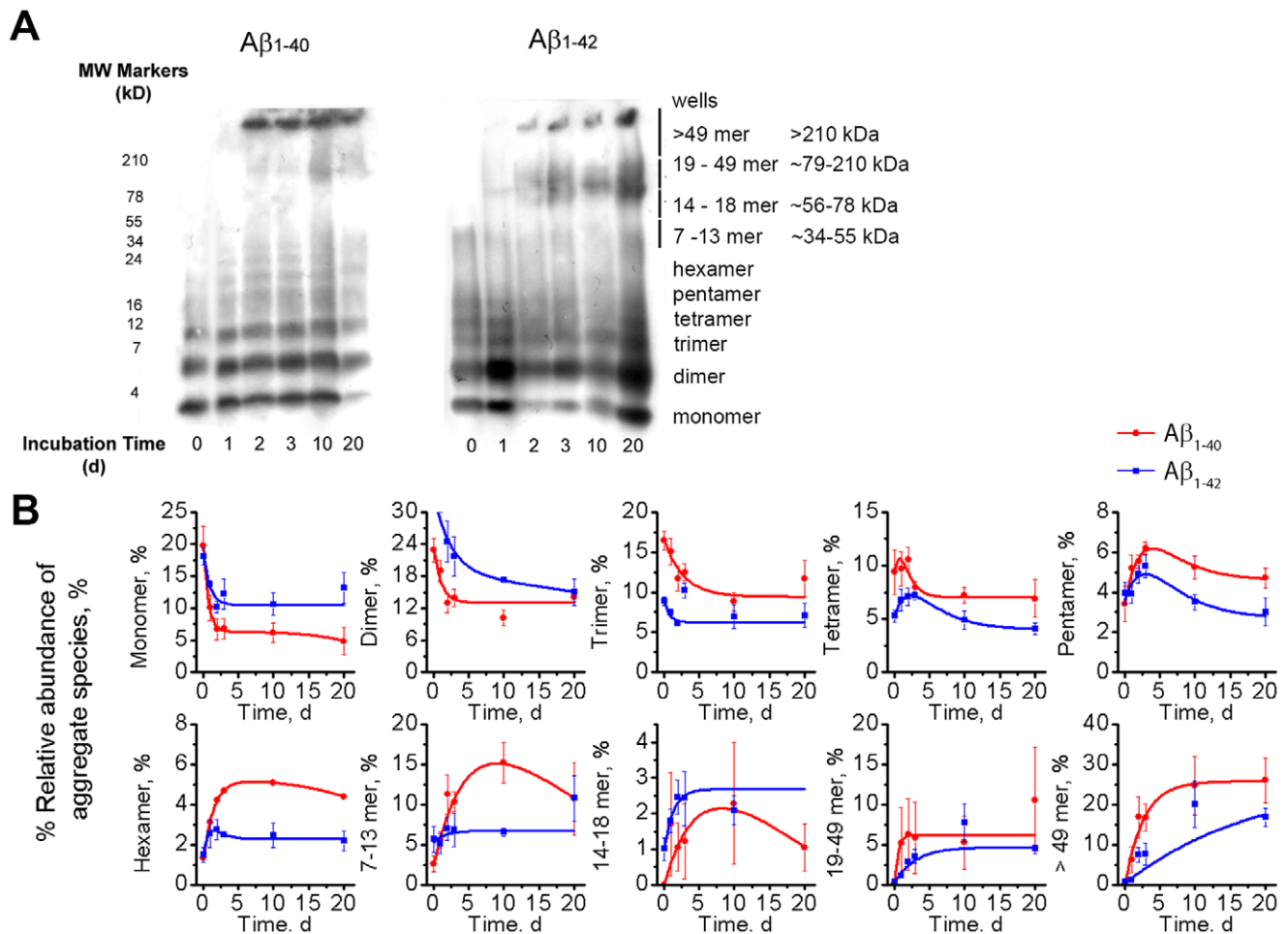


Figure 3. Separation of A β samples by SDS-PAGE followed by Western blot and densitometry analysis. **A)** Example of a Western blot of after SDS-PAGE of A β ₁₋₄₀ (left) and A β ₁₋₄₂ (right) preparations that had been incubated in water for 0, 1, 2, 3, 10, and 20 days (method A). All samples were cross-linked with 12 mM glutaraldehyde before electrophoresis through a 16.5% Tris-Tricine gel. Grouping of oligomers is indicated on the right. **B)** Average relative abundance of aggregated A β ₁₋₄₀ (red) and A β ₁₋₄₂ (blue) species of different size as a function of aggregation time. Each point represents the mean value of the relative abundance of each species from 4 to 6 gels; error bars represent the standard error of the mean. Red and blue curves are best curve fits of equation S1 to the data (see Supporting Information). doi:10.1371/journal.pone.0047261.g003

ometry analysis after Western blot with densitometry analysis after silver staining [83]. Results with A β ₁₋₄₀ showed that both detection techniques revealed similar trends for the change of relative abundance of small oligomer sizes but quantification of abundance for aggregates larger than hexamers was difficult with silver staining, as reported previously (see *Supporting Information*, Fig. S4, and Fig. S5) [83,84]. Silver staining results suggested very low relative amounts of these larger aggregates despite results from TEM analysis, which showed the presence of a significant fraction of A β protofibrils with lengths above 20 nm in three day samples and in samples with longer aggregation time (see *Supporting Information*, Figure S6 and Section S2.5). Therefore, we performed the quantitative analysis of oligomer abundance in this work based on Western blots. The time-dependent variations of the relative amounts of individual A β species as determined by SDS-PAGE (Fig. 3) indicate that this Western-blot-based comparative analysis among differently-aged A β preparations did indeed reveal information about the kinetics of aggregation. Possible artifacts by SDS-induced aggregation [67] or excess aggregation induced by chemical cross-linking [85], if present, were not sufficiently large to mask this time dependence. In fact,

Ono et al. showed that purified samples of cross-linked A β oligomers changed their composition by less than 15% during analysis by SDS-PAGE [23].

Characterization of A β Aggregation by Thioflavin T Fluorescence and Circular Dichroism

We used thioflavin T (ThT) fluorescence as a surrogate to monitor fibrillization [23] and measured circular dichroism (CD) spectra to examine the extent of secondary structure in the samples of A β ₁₋₄₀ and A β ₁₋₄₂ in water after pre-incubation times of 0, 1, 2, 3, 10, and 20 d. The ThT signal from A β ₁₋₄₀ samples reached its half-maximal signal between one and two days ($\tau_{1/2max} = 1.6$ d) and increased only slowly after the third day (Fig. 2C). In case of A β ₁₋₄₂, the half-maximal ThT signal was reached in less than one day ($\tau_{1/2max} = 0.9$ d). Data from CD spectroscopy revealed that the relative amount of β -sheet followed a similar trend as the ThT signal, i.e., a rapid increase during the first 1–2 days, followed by a slower increase as aggregation continued (Fig. 2D and *Supporting Information*, Fig. S7 and Table S2). Together, these ensemble measurements suggested a good correlation between toxicity, ThT fluorescence, and β -sheet content, as reported

previously by Simmons et al [86], while pore formation correlated only during the first three days with ThT fluorescence and β -sheet content. The most pore-forming and most toxic A β preparations were those whose ThT and CD signal transitioned from the initial fast increase to the phase of slow increase.

Dependence of Pore Formation and Cytotoxicity on the Oligomer Populations

In order to develop a model that describes the effect of oligomer populations on pore formation and cytotoxicity, we adopted a multivariate regression approach. This approach is particularly well suited here since we had observations at six time points over twenty days that included the measured levels of pore formation, cytotoxicity, β -sheet content, and ThT fluorescence, as well as the relative abundance of nine different oligomer species for two A β peptides. A multiple linear regression approach might seem logical in this case, but was not appropriate given the relative uncertainties in the explanatory variables (oligomer levels) and response variables (pore formation, cytotoxicity, ThT fluorescence, and β -sheet content) as well as the significant correlations in the oligomer population. Instead, we used a partial least squares (PLS) formalism since it is suited for limited data sets and correlated predictor variables, and has been shown to work well for similar problems ranging from pharmaceuticals to neuroimaging [87–89]. Further, PLS regression does not require any assumptions about the relationship between the observations and the predictor variables, and is ideal for mixtures of species whose predictor variables (i.e., the relative abundance of each oligomer class) contain uncertainty and are interdependent (i.e., tetramer levels depend on trimer and pentamer levels and on the levels of all other oligomer classes in the preparation).

We performed PLS regression using the oligomer abundance as predictor variables and simultaneously carried out regression for all four observables: pore formation, cytotoxicity, β -sheet content, and ThT fluorescence. We carried out this analysis twice by treating data from A β _{1–40} and A β _{1–42} independently and found for each case that a model with two components or latent variables [87] was sufficient to explain 92–95% of the variance of the four observables (see Fig. S8). Interestingly, the component vectors that were obtained for A β _{1–40} and A β _{1–42} are nearly identical, suggesting that the dependence of pore formation, cytotoxicity, β -sheet content, and ThT signal on the underlying oligomer distributions must be similar for both peptides.

Figure 4 shows the PLS regression coefficients for all four observables for A β _{1–40} and A β _{1–42} peptides. In this plot, positive or negative coefficients indicate a positive or negative effect on the given observation, and the asterisks indicate the statistical significance of a given coefficient based on jackknife test [90]. Again we found that both peptides had a nearly identical dependence on the distribution of oligomeric species. In terms of specific observations, cytotoxicity and pore formation had highly correlated dependencies: both had a significant negative contribution from small oligomers (monomers to trimers), significant positive contributions from tetramers to hexamers as well as the 7- to 13-mer group, and then again negative contributions from large oligomers, particularly the >210 kDa class of protofibrils.

These results agree well with previous observations, in particular that the smallest oligomers may in fact be protective rather than pathologic [24,55,91,92], and that oligomers in the tetramer to 13-mer range exert the most significant effect on A β -induced pore formation and toxicity [26,39,44,49,58,61–66]. For instance, Lin et al showed that at least three monomers are required to form A β -induced pores [93], while Pan et al. specifically identified a porin-like, tetrameric β -barrel oligomer in solution and proposed that it

may form ion pores in membranes [65]. Moreover, a recent single molecule microscopy study showed that the dimer to tetramer range of A β _{1–40} constitutes the majority of species binding to neuronal cells at physiological A β concentration and that these binding events were associated with sporadic Ca²⁺ leakage [94]. Bernstein et al. found by ion mobility coupled with mass spectrometry that A β _{1–40} forms stable annular tetramers, while A β _{1–42} forms quasiplanar, annular hexamers as well as dodecamers (from stacking two such hexamers) [39]. Annular oligomers were proposed before as possible pore-forming A β structures [61,68,69,95]. Schauerte et al. combined bilayer experiments with single molecule fluorescence studies and reported that hexamers to 14-mers of A β formed pores [66], while Demuro et al. showed by Ca²⁺-imaging that 5- to 40-mers of A β induced pores for Ca²⁺ in plasma membranes [44]. It is surprising and revealing that PLS analysis on the results from planar lipid bilayer experiments carried out here under significantly different experimental conditions identified the same range of oligomer sizes as pore-forming as those identified by single molecule studies on live cells [44,94]. This agreement between different techniques suggests that similar A β pore structures can form in artificial lipid bilayers and in cellular membranes. Evidence from electrophysiological [44,51,54,96], electron microscopic [69,70], X-ray diffraction [70], NMR [97,98], AFM [56,61], mass spectrometry [39,65], and molecular dynamics experiments [97,99,100] suggests that these A β pore structures are formed by an annular arrangement of several monomers.

In order to further examine the plausibility for the formation of these proposed A β pore structures, we applied a simple barrel-stave model of such an A β pore to estimate the numbers of monomers per pore from single channel recordings of A β -induced ion flux (Fig. 1) and compared these numbers with the results from PLS analysis. This analysis revealed that the theoretically expected single channel conductance values through the lumen of A β pores that form by assembly of four to thirteen A β monomers to a regular polygon of transmembrane cylinders range from 47 pS to 1.2 nS (Fig. S9, Supporting Information). This range is in excellent agreement with the experimentally measured range of 80 pS to 0.8 nS and illustrates that annular arrangements of four to thirteen A β monomers could indeed form ion pores in a size range that is consistent with experimentally measured values of single channel conductance (Fig. S9). In contrast, trimeric assemblies as well as assemblies of more than thirteen A β monomers would have predicted conductance values that are outside of the majority of experimentally measured values according to this simple model (Fig. S9).

The size range from dimers to 8-mers constitutes the predominant A β oligomer fraction in the brain [15] and includes the range of oligomer sizes suspected to be the most clinically relevant in the context of Alzheimer's disease [23]. Injection of purified 9- and 12-mers into the ventricle of pre-trained rats, for instance, had acute effects on spatial memory performance [15]. Finally, Ono et al. reported toxicity studies with cross-linked and purified A β oligomer species [23]. These studies showed the following rank order of increasing and additive toxicity: A β monomers < dimers < trimers < tetramers (larger aggregates were not examined).

Unlike the tetramer to 13-mer range of oligomers, the monomer, dimer, and trimer species were anticorrelated with both pore formation and cytotoxicity (Fig. 4). These findings agree with observations by Schauerte et al. that dimers do not permeabilize membranes and with previous observations that at least three peptides are required to form a pore [66,79,93]. These results deviate, however, from reports that A β dimers are the most toxic species [28–34]. Belinova et al. recently reviewed these

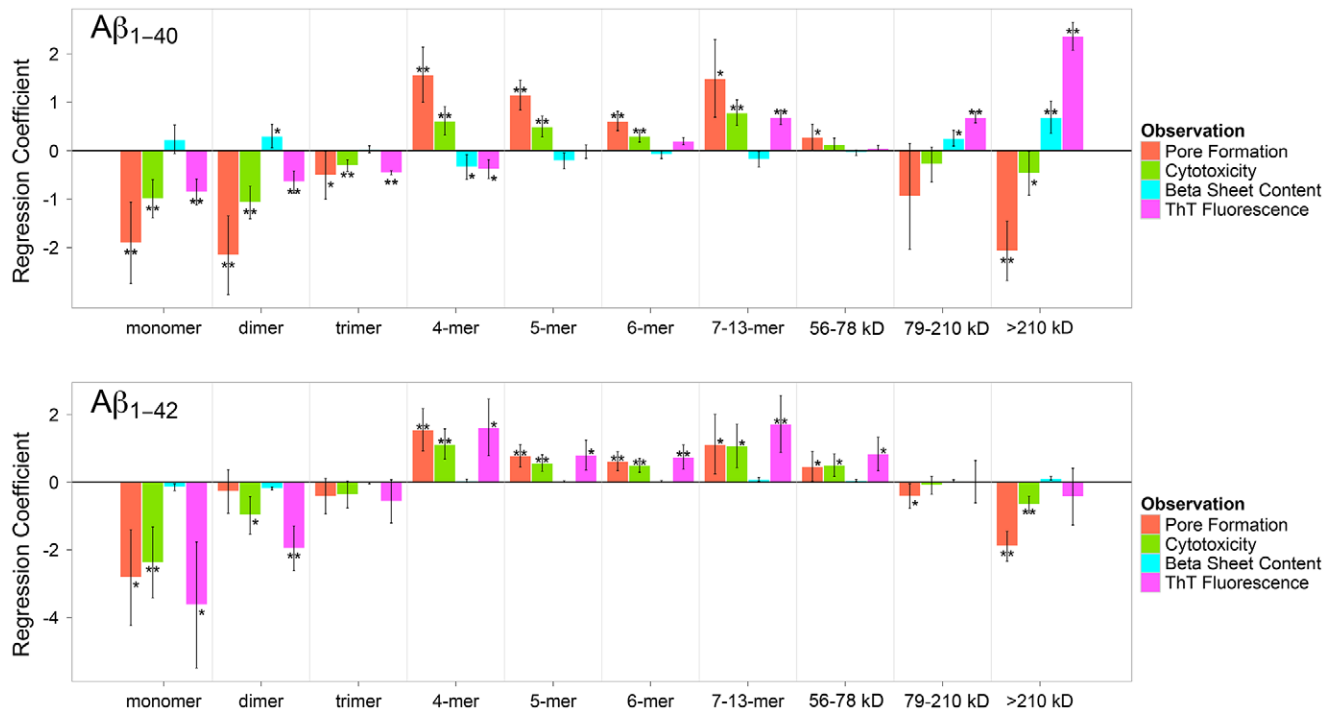


Figure 4. Dependence of pore formation, cytotoxicity, β -sheet content and ThT fluorescence on the oligomer levels of $A\beta_{1-40}$ (top) and $A\beta_{1-42}$ (bottom). The sign of the regression coefficients indicates whether a particular species contributes positively or negatively to a particular observation. The error bars are the standard deviation of the coefficient estimated through a jackknife procedure [90]. Coefficients less than 0.25 were considered insignificant and values that were at least one or two standard deviations from zero are marked as significant (*) or highly significant (**) respectively.

doi:10.1371/journal.pone.0047261.g004

findings and concluded that the identified dimers may aggregate to larger oligomers during toxicity assays and that the observed toxicity may have originated from these larger species [67]. In fact, O’Nuallain confirmed rapid aggregation of these dimers to metastable protofibrils [31].

The observation that large oligomers (>210 kDa) are anticorrelated with pore formation and toxicity, rather than making no contribution, may be explained by recent findings that monomers bind to and dissociate from $A\beta$ oligomers and fibrils in a dynamic process [23,101,102]. Therefore, fibrils (and, presumably, large oligomers) can act as non-toxic scavengers of pore-forming and toxic $A\beta$ species [67] that may otherwise be free to form small toxic oligomers [27,103]. Several recent reports showed that $A\beta$ fibrils are not toxic [13,23,58,103–105]. This close correlation – both, negative and positive – between pore formation and cytotoxicity over the entire size range of both $A\beta$ peptides implies a close mechanistic connection and is consistent with recent findings by Diaz et al. that blockers of $A\beta$ “ion channels” protected cells from $A\beta$ -induced toxicity [106].

Both ThT fluorescence and β -sheet content have little contribution from small and intermediate oligomers in these ensemble measurements – all the coefficients are relatively small and only a few are significant, however, in the case of $A\beta_{1-40}$, both of these observables have strong, positive contributions from the 78–210 kDa and >210 kDa oligomer classes. As one might expect, the β -sheet and ThT signals from these large oligomers are largely correlated, however both observables are anticorrelated with pore formation and cytotoxicity. This result is important since it demonstrates that fibrillization, β -sheet content, pore formation, and toxicity can depend differently on various oligomer species (Fig. 4), although ensemble measurements on mixtures of $A\beta$

species suggest the misleading result that all four observables are correlated with each other (Fig. 2).

Conclusions

One of the proposed mechanisms of $A\beta$ -induced neurotoxicity is pore formation [69,71,107]. Studies from different research groups using various techniques [51–54,56,58–64,66,108] have indicated that aggregated forms of $A\beta$ with a broad range of sizes can induce ion flux through artificial and cellular lipid membranes. One of the big challenges for revealing the pathogenic mechanisms of $A\beta$ is that measurements are performed on a dynamic and distributed ensemble of oligomers [12,109,110]. In fact, it is intrinsically difficult or impossible to perform assays on individual $A\beta$ species because even cross-linked and purified $A\beta$ dimers were reported to form a small fraction of tetramers [23] or larger oligomers during the course of experiments [67,109,110]. Moreover, assays performed on these complex mixtures of $A\beta$ oligomers are usually limited to bulk measurements whose readouts such as cytotoxicity, extent of fibrillization, or β -sheet content may appear to be correlated (Fig. 2), while the biophysical basis for these phenomena may depend on different oligomer species in the mixture (Fig. 4) [67,80]. In order to tackle these complications, we used a PLS formalism that reduced the dimensionality from ten oligomer classes to two component vectors, and made it possible to analyze four observables at six time points simultaneously over a 20 day period. This analysis showed that measures of structure such as β -sheet content or degree of fibrillization depended on different $A\beta$ oligomer species than pore formation and toxicity. Interestingly, pore formation and toxicity showed nearly identical dependence on different species in the oligomer distribution. Moreover, the close connection between pore formation and

toxicity was observed independently for A β ₁₋₄₀ and A β ₁₋₄₂ despite differences in aggregation kinetics (Fig. 2) and relative amounts of aggregated A β species of different size at any given time point (Fig. 3) in these two amyloid preparations [39].

Based on this analysis, we found tetramers to 13-mers contributed positively to pore formation and toxicity and within this range, the tetramer to hexamer populations showed the highest statistical significance for both peptides. This size range is in excellent agreement with previously identified size ranges of A β oligomers as determined by biophysical, computational, and structural studies on pore formation as well as with in-vitro and in-vivo studies of neurotoxicity.

Multivariate PLS analysis also revealed that the smallest (monomer to trimer) and largest A β species (>210 kDa) contributed negatively to pore formation and cytotoxicity and may therefore act as inert sinks that scavenge toxic oligomers [67]. Taken together, these results provide evidence that – under the experimental conditions explored in this work – pore formation was a significant component of cytotoxicity. The tetrameric to hexameric oligomers that we identified as the most pore-forming and toxic oligomers, have been found in the brain of AD patients and it is plausible that they could cause sporadic leaks of calcium ions into neurons [44,94]. These insults, over years of exposure, may contribute to cumulative neuronal damage in Alzheimer's disease.

This study introduces an unbiased, systematic approach to deduce statistical correlations between the size distribution of A β oligomers and pore formation, toxicity, β -sheet content and extent of fibrillization. This multivariate approach is different from previous studies on A β -induced toxicity and pore formation, nonetheless its results agree with many previous findings on A β -induced pore formation or cytotoxicity. This approach therefore supports the idea that A β -induced pore formation may be a significant mechanism of its toxicity. Similar multivariate PLS analyses might be valuable for other amyloidogenic diseases in which standard ensemble measurements often mask the cytotoxic contributions of individual aggregate species in complex and dynamic mixtures of amyloids.

Materials and Methods

Please refer to the Supporting Information for details on chemicals, materials and methods such as formation of lipid bilayers, current recordings, preparation of A β samples, toxicity assays, Western blotting, silver staining, densitometry analysis, ThT fluorescence assays, CD spectrometry, transmission electron microscopy, statistical analysis, partial least squares analysis as well as for Supplementary Results, Tables, and Figures.

Supporting Information

Figure S1 SDS-PAGE/Western blot of A β samples from different suppliers with or without treatment with HFIP followed by lyophilization. All A β samples were prepared freshly in deionized H₂O at a conc. of 1 mg mL⁻¹. Each well in the 18% Tris-HCl gel (Bio-rad) was loaded with 0.2 μ g of A β . Lane 1 = Bachem (non-lyophilized); 2 = GL Biochem, Ltd (Shanghai) (non-lyophilized); 3 = Biopeptide Inc. (non-lyophilized); 4 = GL Biochem, Ltd (Shanghai) (lyophilized); and 5 = Biopeptide Inc. (lyophilized). Aggregation of A β varies in commercial sources. HFIP treatment followed by lyophilization for 2 d removed all aggregates of A β larger than ~ 12 kDa in the case of A β ₁₋₄₀ and removed large A β aggregates (>225 kDa) in the case of A β ₁₋₄₂. (TIF)

Figure S2 19F-NMR spectroscopy of HFIP in CD3OD (left) and A β 1-40 sample that was incubated with HFIP and then lyophilized for two days as described in the Materials and Methods section (right). ¹⁹F resonance of HFIP gave a doublet at -77.8 ppm, while the peak was absent after A β was lyophilized in HFIP for 48 h. (TIF)

Figure S3 SDS-PAGE/Western blotting of cross-linked A β 1-40 and A β 1-42 samples from various preparation methods. 1) Method B: non-HFIP treated A β (GL Biochem, Ltd) in di-H₂O with 0 d incubation; 2) Method C: Modified Kaye preparation; 3) Method D: A β proteoliposomes containing DOPS; and 4) Method E: A β proteoliposomes containing 30% of positively charged DOTAP lipids. The presence of high molecular weight oligomers from these four samples indicates that these preparations accelerated the aggregation of A β compared to preparations in diH₂O (Method A) (e.g. lanes 4 and 5 in Fig. S1) [104,111]. (TIF)

Figure S4 Silver staining after SDS-PAGE of cross-linked A β 1-40 samples prepared by method A for 0 to 20 d. Two micrograms of sample were loaded into each well. The relative amount of intermediate aggregates (dimers to hexamers) or large aggregates of A β (the species in lane 10 and 20 in the stacking gel) increased with incubation time. The stacking portion of the silver stained gel appeared with a dark background even in the absence of protein (blank) as shown in the first lane on the left of the gel, making quantitative analysis of large aggregates by silver staining difficult. (TIF)

Figure S5 Relative abundance of various cross-linked A β 1-40 aggregates of different size obtained after SDS-PAGE and silver staining. The intensity on the gel was corrected by subtraction of the blank (in the absence of protein). Each point represents the average of relative abundance of aggregates from six independent gels and samples; error bars represent the standard error of the mean. Red curves are best fits of equation (S1) to the data. (TIF)

Figure S6 Transmission electron micrographs of A β 1-40 aggregates. Micrographs were taken of A β ₁₋₄₀ aggregates after the aggregates had been incubated for zero, one, two, or three days according to Method A. Two micrographs are shown for each day, each taken at different locations on the TEM grid. (TIF)

Figure S7 Circular dichroism spectra of A β 1-40 (left panel) and A β 1-42 (right panel) samples prepared by method A as a function of incubation time. With increasing incubation time, the A β -sheet content in A β samples increased, while the random coil content decreased. (TIF)

Figure S8 Loadings of the first and second components (latent variables) for both A β peptides as determined by PLS regression. The first components for A β ₁₋₄₀ and A β ₁₋₄₂ (solid lines) and the second components for A β ₁₋₄₀ and A β ₁₋₄₂ (dotted lines) are nearly identical and have inner products of 0.91 and 0.87, respectively. The percentages listed indicate the percent of the variance explained by each component. These results indicate that the relationship between the four observables and the oligomer ensemble must be similar for the two peptides. (TIF)

Figure S9 Comparison of experimentally measured single channel conductance values of A β 1–40 pores with theoretically predicted values.

These box plots were constructed from the amplitude of single-step current jumps in current *versus* time traces such as those shown in Fig. 1 of the main text. The first six box plots (A β 40-0d to A β 40-20d) represent the distribution of single channel conductance values from A β preparations that had been pre-incubated for 0 to 20 days prior to planar lipid bilayer recordings under the same conditions as in Fig 1 of the main text. The last box plot (dark yellow) represents the theoretical estimate of single channel conductance values of a model of A β pores that assumes an annular assembly of A β monomers to a regular polygon with an internal pore lumen. In this model, each A β monomer is represented by a transmembrane cylinder with a diameter, d , of 1 nm (approximate diameter of a transmembrane peptide) [112] and a length, l , of 3.5 nm (approximate thickness of a lipid bilayer). The centers of the cross-section of each cylinder are located at the corners of the regular polygon and the lengths of the polygon sides are equal to d . The theoretically predicted box plot was constructed from estimated single channel conductance values of eleven possible regular polygons ranging from the smallest one (assembly of three monomers to a triangle) to a regular polygon of 13 monomers. We estimated the single channel conductance as a function of the number of A β monomers, N , in these assemblies by calculating the area of the lumen $A_L(N)$ in such a pore. We obtained this area by calculating the area of a regular polygon with N sides, $A_{RP}(N)$ and subtracting the area of circle sectors, $A_{CS}(N)$, that overlap with the polygon area. The area of a regular polygon is given by: $A_{RP}(N) = d^2 \times N / [4 \times \tan(180^\circ / N)]$ and the area of circle sectors depends on the angle, α , between the sides of a regular polygon – which is given by $\alpha(N) = 180^\circ (N - 2) / N$ – in the following way: $A_{CS}(N) = \alpha(N) \times \pi \times d^2 / (4 \times 360^\circ)$. Therefore, the area of the lumen is given by: $A_L(N) = A_{RP}(N) - N \times A_{CS}(N) = (d^2 / 4) \times [N / \tan(180^\circ / N) - (\pi / 2) \times (N - 2)]$. With $A_L(N)$, we calculated the area equivalent radius of a circle as a function of the number of monomers, $r(N)$, i.e. $r(N) = (A_L(N) / \pi)^{0.5}$, which we then used to calculate the single

channel conductance, $\gamma(N)$, through a pore with radius $r(N)$ and length l in an electrolyte with resistivity ρ using the relationship $\gamma(N) = [(l + \pi \times r(N) / 2) \times \rho / [\pi \times r^2(N)]]^{-1}$ [113]. Since we used a lipid bilayer with 50 mol% negatively-charged lipid head groups, we estimated the local resistivity near the membrane from work by Apell *et al* [114] and found $\rho = 0.313 \Omega \text{ m}$ for the experimental conditions used in Fig. 1 of the main text. The predicted box plot (dark yellow) was then obtained from the $\gamma(N)$ values of oligomers with 3 to 13 monomers, weighed by the relative abundance of each of these oligomers as shown in Fig. 3B of the main text. In these plots, the box encloses the 25th to 75th percentile, the whiskers enclose the 5th to 95th percentile, the crosses enclose the 1st to 99th percentile, the hyphens indicate the minimum and maximum single channel conductance value, while the horizontal line in the box indicates the median and the open square symbol indicates the mean single channel conductance value.

(TIF)

Table S1 Comparison of different A β aggregation procedures with regard to the propensity of the resulting A β preparation to form pores in planar lipid bilayers and to kill cells.

(DOCX)

Table S2 Deconvolution of CD spectra of A β in different preparation methods.

(DOCX)

Acknowledgments

We thank Ricardo Capone for help with the first experiments.

Author Contributions

Conceived and designed the experiments: PP JY MM. Performed the experiments: PP ECY. Analyzed the data: DS JY MM. Contributed reagents/materials/analysis tools: DS MM. Wrote the paper: PP ECY DS JY MM.

References

- Selkoe DJ (1991) The molecular pathology of Alzheimer's disease. *Neuron* 6: 487–498.
- Hardy JA, Higgins GA (1992) Alzheimer's disease - the amyloid cascade hypothesis. *Science* 256: 184–185.
- LaFerla FM, Green KN, Oddo S (2007) Intracellular amyloid- β in Alzheimer's disease. *Nature Reviews Neuroscience* 8: 499–509.
- Glenner GG, Wong CW (1984) Alzheimer's disease - initial report of the purification and characterization of a novel cerebrovascular amyloid protein. *Biochemical and Biophysical Research Communications* 120: 885–890.
- Wong CW, Quaranta V, Glenner GG (1985) Neuritic plaques and cerebrovascular amyloid in Alzheimer's disease are antigenically related. *Proceedings of the National Academy of Sciences of the United States of America* 82: 8729–8732.
- Hardy J, Selkoe DJ (2002) The amyloid hypothesis of Alzheimer's disease: progress and problems on the road to therapeutics. *Science* 297: 353–356.
- Mattson MP (2004) Pathways towards and away from Alzheimer's disease. *Nature* 430: 631–639.
- Rangachari V, Reed DK, Moore BD, Rosenberry TL (2006) Secondary structure and interfacial aggregation of amyloid- β (1–40) on sodium dodecyl sulfate micelles. *Biochemistry* 45: 8639–8648.
- Querfurth HW, LaFerla FM (2010) Mechanisms of disease: Alzheimer's disease. *New England Journal of Medicine* 362: 329–344.
- Parihar MS, Hemnani T (2004) Alzheimer's disease pathogenesis and therapeutic interventions. *Journal of Clinical Neuroscience* 11: 456–467.
- Habib LK, Lee MTC, Yang J (2010) Inhibitors of catalase-amyloid interactions protect cells from β -amyloid-induced oxidative stress and toxicity. *Journal of Biological Chemistry* 285: 38933–38943.
- Eisenberg D, Jucker M (2012) The amyloid state of proteins in human diseases. *Cell* 148: 1188–1203.
- Lansbury PT, Lashuel HA (2006) A century-old debate on protein aggregation and neurodegeneration enters the clinic. *Nature* 443: 774–779.
- Selkoe DJ (2011) Resolving controversies on the path to Alzheimer's therapeutics. *Nature Medicine* 17: 1060–1065.
- Walsh DM, Selkoe DJ (2007) A β Oligomers - a decade of discovery. *Journal of Neurochemistry* 101: 1172–1184.
- Gong YS, Chang L, Viola KL, Lacor PN, Lambert MP, et al. (2003) Alzheimer's disease-affected brain: presence of oligomeric β ligands (ADDLs) suggests a molecular basis for reversible memory loss. *Proceedings of the National Academy of Sciences of the United States of America* 100: 10417–10422.
- LaFerla FM (2002) Calcium dyshomeostasis and intracellular signalling in Alzheimer's disease. *Nature Reviews Neuroscience* 3: 862–872.
- Lambert MP, Barlow AK, Chromy BA, Edwards C, Freed R, et al. (1998) Diffusible, nonfibrillar ligands derived from A β (1–42) are potent central nervous system neurotoxins. *Proceedings of the National Academy of Sciences of the United States of America* 95: 6448–6453.
- Small DH, Mok SS, Bornstein JC (2001) Alzheimer's disease and A β toxicity: from top to bottom. *Nature Reviews Neuroscience* 2: 595–598.
- Turner PR, O'Connor K, Tate WP, Abraham WC (2003) Roles of amyloid precursor protein and its fragments in regulating neural activity, plasticity and memory. *Progress in Neurobiology* 70: 1–32.
- Bucciantini M, Giannoni E, Chiti F, Baroni F, Formigli L, et al. (2002) Inherent toxicity of aggregates implies a common mechanism for protein misfolding diseases. *Nature* 416: 507–511.
- Khachaturian ZS (1987) Hypothesis on the regulation of cytosol calcium concentration and the aging brain. *Neurobiology of Aging* 8: 345–346.
- Ono K, Condron MM, Teplow DB (2009) Structure-neurotoxicity relationships of amyloid β -protein oligomers. *Proceedings of the National Academy of Sciences of the United States of America* 106: 14745–14750.
- Demuro A, Mina E, Kaye R, Milton SC, Parker I, et al. (2005) Calcium dysregulation and membrane disruption as a ubiquitous neurotoxic mechanism of soluble amyloid oligomers. *Journal of Biological Chemistry* 280: 17294–17300.

25. Holtzman DM, Goate A, Kelly J, Sperling R (2011) Mapping the road forward in Alzheimer's disease. *Science Translational Medicine* 3.
26. Pike CJ, Burdick D, Walencewicz AJ, Glabe CG, Cotman CW (1993) Neurodegeneration induced by β -amyloid peptides in vitro: the role of peptide assembly state. *Journal of Neuroscience* 13: 1676–1687.
27. Broersen K, Rousseau F, Schymkowitz J (2010) The culprit behind amyloid beta peptide related neurotoxicity in Alzheimer's disease: oligomer size or conformation? *Alzheimers Res Ther* 2: 12.
28. Klyubin I, Betts V, Welzel AT, Blennow K, Zetterberg H, et al. (2008) Amyloid β protein dimer-containing human CSF disrupts synaptic plasticity: prevention by systemic passive immunization. *Journal of Neuroscience* 28: 4231–4237.
29. Shankar GM, Leissring MA, Adame A, Sun X, Spooner E, et al. (2009) Biochemical and immunohistochemical analysis of an Alzheimer's disease mouse model reveals the presence of multiple cerebral A β assembly forms throughout life. *Neurobiology of Disease* 36: 293–302.
30. Shankar GM, Li SM, Mehta TH, Garcia-Munoz A, Shepardson NE, et al. (2008) Amyloid- β protein dimers isolated directly from Alzheimer's brains impair synaptic plasticity and memory. *Nature Medicine* 14: 837–842.
31. O'Nuallain B, Freir DB, Nicoll AJ, Risse E, Ferguson N, et al. (2010) Amyloid β -protein dimers rapidly form stable synaptotoxic protofibrils. *Journal of Neuroscience* 30: 14411–14419.
32. Podlisy MB, Ostaszewski BL, Squazzo SL, Koo EH, Rydell RE, et al. (1995) Aggregation of secreted amyloid β -protein into sodium dodecyl sulfate-stable oligomers in cell culture. *Journal of Biological Chemistry* 270: 9564–9570.
33. Jin M, Shepardson N, Yang T, Chen G, Walsh D, et al. (2011) Soluble amyloid β -protein dimers isolated from Alzheimer cortex directly induce tau hyperphosphorylation and neuritic degeneration. *Proceedings of the National Academy of Sciences of the United States of America* 108: 5819–5824.
34. Nussbaum JM, Schilling S, Cynis H, Silva A, Swanson E, et al. (2012) Prion-like behaviour and tau-dependent cytotoxicity of pyroglutamylated amyloid- β . *Nature advance online publication*. doi:10.1038/nature11060.
35. Townsend M, Shankar GM, Mehta T, Walsh DM, Selkoe DJ (2006) Effects of secreted oligomers of amyloid β -protein on hippocampal synaptic plasticity: a potent role for trimers. *Journal of Physiology* 572: 477–492.
36. Viola KL, Velasco PT, Klein WL (2008) Why Alzheimer's is a disease of memory: the attack on synapses by A β oligomers (ADDLs). *Journal of Nutrition Health & Aging* 12: 51S–57S.
37. Lambert MP, Velasco PT, Chang L, Viola KL, Fernandez S, et al. (2007) Monoclonal antibodies that target pathological assemblies of A β . *Journal of Neurochemistry* 100: 23–35.
38. Hepler RW, Grimm KM, Nahas DD, Breese R, Dodson EC, et al. (2006) Solution state characterization of amyloid β -derived diffusible ligands. *Biochemistry* 45: 15157–15167.
39. Bernstein SL, Dupuis NF, Lazo ND, Wytenbach T, Condrum MM, et al. (2009) Amyloid- β protein oligomerization and the importance of tetramers and dodecamers in the aetiology of Alzheimer's disease. *Nature Chemistry* 1: 326–331.
40. Lesne S, Koh MT, Kotilinek L, Kaye R, Glabe CG, et al. (2006) A specific amyloid-beta protein assembly in the brain impairs memory. *Nature* 440: 352–357.
41. Harper JD, Wong SS, Lieber CM, Lansbury PT (1997) Observation of metastable A β amyloid protofibrils by atomic force microscopy. *Chemistry & Biology* 4: 119–125.
42. Walsh DM, Lomakin A, Benedek GB, Condrum MM, Teplow DB (1997) Amyloid β -protein fibrillogenesis - detection of a protofibrillar intermediate. *Journal of Biological Chemistry* 272: 22364–22372.
43. Kaye R, Pensalfini A, Margol L, Sokolov Y, Sarsoza F, et al. (2009) Annular protofibrils are a structurally and functionally distinct type of amyloid oligomer. *Journal of Biological Chemistry* 284: 4230–4237.
44. Demuro A, Smith M, Parker I (2011) Single-channel Ca²⁺ imaging implicates A β 1–42 amyloid pores in Alzheimer's disease pathology. *Journal of Cell Biology* 195: 515–524.
45. Puzzo D, Arancio O (2006) Fibrillar β -amyloid impairs the late phase of long term potentiation. *Current Alzheimer Research* 3: 179–183.
46. Lorenzo A, Yuan ML, Zhang ZH, Paganetti PA, Sturchler-Pierrat C, et al. (2000) Amyloid β interacts with the amyloid precursor protein: a potential toxic mechanism in Alzheimer's disease. *Nature Neuroscience* 3: 460–464.
47. Chen QS, Kagan BL, Hirakura Y, Xie CW (2000) Impairment of hippocampal long-term potentiation by Alzheimer amyloid β -peptides. *Journal of Neuroscience Research* 60: 65–72.
48. Soscia SJ, Kirby JE, Washicosky KJ, Tucker SM, Ingelsson M, et al. (2010) The Alzheimer's disease-associated amyloid β -protein is an antimicrobial peptide. *PLoS ONE* 5.
49. Williams TL, Serpell LC (2011) Membrane and surface interactions of Alzheimer's A β peptide - Insights into the mechanism of cytotoxicity. *FEBS Journal* 278: 3905–3917.
50. Wong PT, Schauerte JA, Wissner KC, Ding H, Lee EL, et al. (2009) Amyloid- β membrane binding and permeabilization are distinct processes influenced separately by membrane charge and fluidity. *Journal of Molecular Biology* 386: 81–96.
51. Arispe N, Pollard HB, Rojas E (1993) Giant multilevel cation channels formed by Alzheimer-disease amyloid beta-protein [A β -P(1–40)] in bilayer membranes. *Proceedings of the National Academy of Sciences of the United States of America* 90: 10573–10577.
52. Jang H, Zheng J, Nussinov R (2007) Models of β -amyloid ion channels in the membrane suggest that channel formation in the bilayer is a dynamic process. *Biophysical Journal* 93: 1938–1949.
53. Kagan BL, Azimov R, Azimova R (2004) Amyloid peptide channels. *Journal of Membrane Biology* 202: 1–10.
54. Capone R, Quiroz FG, Prangko P, Saluja I, Sauer AM, et al. (2009) Amyloid- β -induced ion flux in artificial lipid bilayers and neuronal cells: resolving a controversy. *Neurotoxicity Research* 16: 1–13.
55. Caughey B, Lansbury PT (2003) Protofibrils, pores, fibrils, and neurodegeneration: Separating the responsible protein aggregates from the innocent bystanders. *Annual Review of Neuroscience* 26: 267–298.
56. Lal R, Lin H, Quist AP (2007) Amyloid beta ion channel: 3D structure and relevance to amyloid channel paradigm. *Biochimica Et Biophysica Acta-Biomembranes* 1768: 1966–1975.
57. Arispe N, Diaz JC, Simakova O (2007) A β ion channels. Prospects for treating Alzheimer's disease with A β channel blockers. *Biochimica Et Biophysica Acta-Biomembranes* 1768: 1952–1965.
58. Kawahara M (2010) Neurotoxicity of β -amyloid protein: oligomerization, channel formation and calcium dyshomeostasis. *Current Pharmaceutical Design* 16: 2779–2789.
59. Hartley DM, Walsh DM, Ye CPP, Diehl T, Vasquez S, et al. (1999) Protofibrillar intermediates of amyloid β -protein induce acute electrophysiological changes and progressive neurotoxicity in cortical neurons. *Journal of Neuroscience* 19: 8876–8884.
60. Jang H, Arce FT, Capone R, Ramachandran S, Lal R, et al. (2009) Misfolded amyloid ion channels present mobile β -sheet subunits in contrast to conventional ion channels. *Biophysical Journal* 97: 3029–3037.
61. Quist A, Doudevski I, Lin H, Azimova R, Ng D, et al. (2005) Amyloid ion channels: a common structural link for protein-misfolding disease. *Proceedings of the National Academy of Sciences of the United States of America* 102: 10427–10432.
62. Lin H, Bhatia R, Lal R (2001) Amyloid β protein forms ion channels: implications for Alzheimer's disease pathophysiology *Faseb Journal* 15: 2433–2444.
63. Strodel B, Lee JW, Whittleston CS, Wales DJ (2010) Transmembrane structures for Alzheimer's A β (1–42) oligomers. *Journal of the American Chemical Society* 132: 13300–13312.
64. Shafir Y, Durell S, Arispe N, Guy HR (2010) Models of membrane-bound Alzheimer's A β peptide assemblies. *Proteins-Structure Function and Bioinformatics* 78: 3473–3487.
65. Pan J, Han J, Borchers CH, Konermann L (2012) Structure and dynamics of small soluble A β (1–40) oligomers studied by top-down hydrogen exchange mass spectrometry. *Biochemistry* 51: 3694–3703.
66. Schauerte JA, Wong PT, Wissner KC, Ding H, Steel DG, et al. (2010) Simultaneous single-molecule fluorescence and conductivity studies reveal distinct classes of A β species on lipid bilayers. *Biochemistry* 49: 3031–3039.
67. Benilova I, Karran E, De Strooper B (2012) The toxic A β oligomer and Alzheimer's disease: an emperor in need of clothes. *Nature Neuroscience* 15: 349–357.
68. Laganowsky A, Liu C, Sawaya MR, Whitelegge JP, Park J, et al. (2012) Atomic view of a toxic amyloid small oligomer. *Science* 335: 1228–1231.
69. Lashuel HA, Hartley D, Petre BM, Walz T, Lansbury PT (2002) Neurodegenerative disease - amyloid pores from pathogenic mutations. *Nature* 418: 291–291.
70. Stroud JC, Liu C, Teng PK, Eisenberg D (2012) Toxic fibrillar oligomers of amyloid- β have cross- β structure. *Proceedings of the National Academy of Sciences of the United States of America*.
71. Arispe N, Rojas E, Pollard HB (1993) Alzheimer disease amyloid β protein forms calcium channels in bilayer membranes: blockade by tromethamine and aluminum. *Proceedings of the National Academy of Sciences of the United States of America* 90: 567–571.
72. Bhatia R, Lin H, Lal R (2000) Fresh and globular amyloid β protein (1–42) induces rapid cellular degeneration: evidence for A β P channel-mediated cellular toxicity. *FASEB Journal* 14: 1233–1243.
73. Hirakura Y, Lin MC, Kagan BL (1999) Alzheimer amyloid A β 1–42 channels: effects of solvent, pH, and Congo Red. *Journal of Neuroscience Research* 57: 458–466.
74. Kagan BL, Hirakura Y, Azimov R, Azimova R, Lin MC (2002) The channel hypothesis of Alzheimer's disease: current status. *Peptides* 23: 1311–1315.
75. Kourie J, Henry C, Farrelly P (2001) Diversity of amyloid β protein fragment [1–40]-formed channels. *Cellular and Molecular Neurobiology* 21: 255–284.
76. Micelli S, Meleleo D, Picciarelli V, Gallucci E (2004) Effect of sterols on β -amyloid peptide (A β 1–40) channel formation and their properties in planar lipid membranes. *Biophysical Journal* 86: 2231–2237.
77. Arispe N, Pollard HB, Rojas E (1996) Zn²⁺ interaction with Alzheimer amyloid beta protein calcium channels. *Proceedings of the National Academy of Sciences of the United States of America* 93: 1710–1715.
78. Kawahara M, Arispe N, Kuroda Y, Rojas E (1997) Alzheimer's disease amyloid beta-protein forms Zn²⁺-sensitive, cation-selective channels across excised membrane patches from hypothalamic neurons. *Biophysical Journal* 73: 67–75.
79. Kagan BL (2012) Membrane pores in the pathogenesis of neurodegenerative disease. *Progress in molecular biology and translational science* 107: 295–325.

80. Campioni S, Mannini B, Zampagni M, Pensalfini A, Parrini C, et al. (2010) A causative link between the structure of aberrant protein oligomers and their toxicity. *Nature Chemical Biology* 6: 140–147.
81. Majd S, Yusko EC, Billeh YN, Macrae MX, Yang J, et al. (2010) Applications of biological pores in nanomedicine, sensing, and nanoelectronics. *Current Opinion in Biotechnology* 21: 439–476.
82. Wogulis M, Wright S, Cunningham D, Chilcote T, Powell K, et al. (2005) Nucleation-dependent polymerization is an essential component of amyloid-mediated neuronal cell death. *Journal of Neuroscience* 25: 1071–1080.
83. Ryan DA, Narrow WC, Federoff HJ, Bowers WJ (2010) An improved method for generating consistent soluble amyloid-beta oligomer preparations for in vitro neurotoxicity studies. *Journal of Neuroscience Methods* 190: 171–179.
84. Freir DB, Nicoll AJ, Klyubin I, Panico S, Mc Donald JM, et al. (2011) Interaction between prion protein and toxic amyloid β assemblies can be therapeutically targeted at multiple sites. *Nat Commun* 2: 336.
85. Bitan G, Lomakin A, Teplow DB (2001) Amyloid β -protein oligomerization - prenucleation interactions revealed by photo-induced cross-linking of unmodified proteins. *Journal of Biological Chemistry* 276: 35176–35184.
86. Simmons LK, May PC, Tomaselli KJ, Rydel RE, Fuson KS, et al. (1994) Secondary structure of amyloid- β peptide correlates with neurotoxic activity in vitro. *Molecular Pharmacology* 45: 373–379.
87. Boulesteix A-L, Strimmer K (2007) Partial least squares: a versatile tool for the analysis of high-dimensional genomic data. *Briefings in Bioinformatics* 8: 32–44.
88. Krishnan A, Williams LJ, McIntosh AR, Abdi H (2011) Partial least squares (PLS) methods for neuroimaging: a tutorial and review. *Neuroimage* 56: 455–475.
89. Rajalahti T, Kvalheim OM (2011) Multivariate data analysis in pharmaceuticals: a tutorial review. *International Journal of Pharmaceutics* 417: 280–290.
90. Shao J, Tu D (1995) *The jackknife and bootstrap*. New York: Springer.
91. Giuffrida ML, Caraci F, Pignataro B, Cataldo S, De Bona P, et al. (2009) β -amyloid monomers are neuroprotective. *Journal of Neuroscience* 29: 10582–10587.
92. Baruch-Suchodolsky R, Fischer B (2009) $A\beta_{10}$, either soluble or aggregated, is a remarkably potent antioxidant in cell-free oxidative systems. *Biochemistry* 48: 4354–4370.
93. Lin MCA, Kagan BL (2002) Electrophysiologic properties of channels induced by A beta 25–35 in planar lipid bilayers. *Peptides* 23: 1215–1228.
94. Johnson RD, Schauerte JA, Wissner KC, Gafni A, Steel DG (2011) Direct observation of single amyloid- β (1–40) oligomers on live cells: binding and growth at physiological concentrations. *PLoS ONE* 6.
95. Lashuel HA, Lansbury PT (2006) Are amyloid diseases caused by protein aggregates that mimic bacterial pore-forming toxins? *Quarterly Reviews of Biophysics* 39: 167–201.
96. Kagan BL, Jang H, Capone R, Arce FT, Ramachandran S, et al. (2012) Antimicrobial properties of amyloid peptides. *Molecular Pharmaceutics* 9: 708–717.
97. Jang H, Arce FT, Ramachandran S, Capone R, Lal R, et al. (2010) beta-Barrel Topology of Alzheimer's beta-Amyloid Ion Channels. *Journal of Molecular Biology* 404: 917–934.
98. Strodel B, Lee JW, Whittleston CS, Wales DJ (2010) Transmembrane Structures for Alzheimer's A beta(1–42) Oligomers. *Journal of the American Chemical Society* 132: 13300–13312.
99. Connelly L, Jang H, Arce FT, Capone R, Koder SA, et al. (2012) Atomic Force Microscopy and MD Simulations Reveal Pore-Like Structures of All-D-Enantiomer of Alzheimer's beta-Amyloid Peptide: Relevance to the Ion Channel Mechanism of AD Pathology. *Journal of Physical Chemistry B* 116: 1728–1735.
100. Jang HB, Zheng J, Lal R, Nussinov R (2008) New structures help the modeling of toxic amyloid beta ion channels. *Trends in Biochemical Sciences* 33: 91–100.
101. Sanchez L, Madurga S, Pukala T, Vilaseca M, Lopez-Iglesias C, et al. (2011) $A\beta_{40}$ and $A\beta_{42}$ amyloid fibrils exhibit distinct molecular recycling properties. *Journal of the American Chemical Society* 133: 6505–6508.
102. Bitan G, Kirkitadze MD, Lomakin A, Vollers SS, Benedek GB, et al. (2003) Amyloid β -protein ($A\beta$) assembly: $A\beta_{40}$ and $A\beta_{42}$ oligomerize through distinct pathways. *Proceedings of the National Academy of Sciences of the United States of America* 100: 330–335.
103. Demuro A, Parker I, Stutzmann GE (2010) Calcium signaling and amyloid toxicity in Alzheimer's disease. *Journal of Biological Chemistry* 285: 12463–12468.
104. Butterfield SM, Lashuel HA (2010) Amyloidogenic protein membrane interactions: mechanistic insight from model systems. *Angewandte Chemie-International Edition* 49: 5628–5654.
105. Schnabel J (2011) Amyloid: little proteins, big clues. *Nature* 475: S12–S14.
106. Diaz JC, Simakova O, Jacobson KA, Arispe N, Pollard HB (2009) Small molecule blockers of the Alzheimer $A\beta$ calcium channel potently protect neurons from $A\beta$ cytotoxicity. *Proceedings of the National Academy of Sciences of the United States of America* 106: 3348–3353.
107. Marx J (2007) Alzheimer's disease - Fresh evidence points to an old suspect: calcium. *Science* 318: 384–385.
108. Arispe NJ, Simakova O (2007) Alzheimer's disease $A\beta$ peptide binding to cell membranes is correlated to membrane surface phosphatidylserine levels. *Biophysical Journal*: 612A–612A.
109. Bitan G, Fradinger EA, Spring SM, Teplow DB (2005) Neurotoxic protein oligomers - what you see is not always what you get. *Amyloid-Journal of Protein Folding Disorders* 12: 88–95.
110. Ding H, Wong PT, Lee EL, Gafni A, Steel DG (2009) Determination of the oligomer size of amyloidogenic protein β -amyloid(1–40) by single-molecule spectroscopy. *Biophysical Journal* 97: 912–921.
111. Kurganov B, Doh M, Arispe N (2004) Aggregation of liposomes induced by the toxic peptides Alzheimer's $A\beta$ s, human amylin and prion (106–126): facilitation by membrane-bound GM1 ganglioside. *Peptides* 25: 217–232.
112. Mayer M, Semetey V, Gitlin I, Yang J, Whitesides GM (2008) Using ion channel-forming peptides to quantify protein-ligand interactions. *Journal of the American Chemical Society* 130: 1453–1465.
113. Hille B (2001) *Ion channels of excitable membranes*. Sunderland: Sinauer Associates, Inc.
114. Apell HJ, Bamberg E, Lauger P (1979) Effects of Surface-Charge on the Conductance of the Gramicidin Channel. *Biochimica Et Biophysica Acta* 552: 369–378.